Cell Reports, Volume *23*

Supplemental Information

Dorsolateral Striatum Engagement Interferes with Early Discrimination Learning

Hadley C. Bergstrom, Anna M. Lipkin, Abby G. Lieberman, Courtney R. Pinard, Ozge Gunduz-Cinar, Emma T. Brockway, William W. Taylor, Mio Nonaka, Olena Bukalo, Tiffany A. Wills, F. Javier Rubio, Xuan Li, Charles L. Pickens, Danny G. Winder, and Andrew Holmes

Supplemental Experimental Procedures

Subjects

Unless stated otherwise, subjects were male C57BL/6J mice obtained from The Jackson Laboratory (Bar Harbor, ME, USA) grouped housed prior to surgery, then singly housed (to maintain the integrity of intra-cranial implants) in a temperature and humidity controlled vivarium under a 12-hour light/dark cycle (lights on 0600 h). Experimental procedures were performed in accordance with the National Institutes of Health Guide for Care and Use of Laboratory Animals and approved by the local NIAAA Animal Care and Use Committee. The number of mice used in each experiment is indicated in the Results.

Behavioral task

General testing procedures were based on those previously reported (Brigman et al., 2013; Graybeal et al., 2011; Horner et al., 2013; Izquierdo et al., 2006) and used the Bussey-Saksida Touch Screen System (model 80614, Lafayette Instruments, Lafayette, IN, USA). Prior to testing, body weight was reduced and maintained at 85% free feeding weight throughout testing to motivate responding. Mice were first familiarized with ~10 reward pellets/mouse in the home cage and, the following day, acclimated to the test chambers for 30 minutes with access to 10 x 14 mg pellets (#F05684, BioServ, Frenchtown, NJ, USA) in the food magazine. Mice were next trained to associate the dispensing of reward with a magazine light and an auditory cue. Thirty pellets were randomly dispensed and the presentation of the reward was concurrent with the presentation of a 2-second, 65-dB tone and illumination of the magazine light. Mice that consumed all pellets in a 30-minute session proceeded to instrumental pre-training, which entailed 3 successive phases.

In phase 1, the mouse was required to initiate each trial with a head entry into the food magazine upon illumination, which extinguished the magazine light and resulted in the appearance of a 6.5 cm^2 stimulus (selected randomly from a catalogue) in 1 of the 2 touchscreen windows for 10 seconds. When the stimulus disappeared, a 1-pellet reward was delivered, in conjunction with the tone and magazine light cues. Touches at the window containing the stimulus earned 1 pellet to encourage responding. The criterion for phase 1 was earning 30 pellets in <30 minutes. In phase 2, a stimulus was presented in 1 of the 2 stimulus windows and the mouse was required to touch the window containing the stimulus to receive a reward. The criterion for phase 2 was earning 30 pellets in <30 minutes. Phase 3 was the same as phase 2 with the exception that, to discourage indiscriminate touchscreen responding, touches at a blank window led to a 15-second 'timeout' period during which the house light was extinguished and a new trial could not be initiated. Following a blank-screen response, a 'correction trial' was given in which the same stimulus was presented in the same window. The next trial proper could not begin until a stimulus-window response was made on a correction trial. There were 30 trials proper per session/day. The criterion for phase 3 was touching the stimulus-containing screen on >75% of trials.

For discrimination learning, 2 novel 6.5 cm^2 stimuli ('fan' and 'marbles') were presented simultaneously. Responses at the 'fan' stimulus produced a food reward at a continuous rate of reinforcement. Responses at the 'marble' stimulus (='errors') produced no food reward and a 15-second 'timeout' period. Because there is an unconditioned perceptual bias towards the 'marble' stimulus at the beginning of training, this stimulus-reward contingency represents a biased design. . Each error was followed by a correction trial in which the 2 stimuli were presented in the same spatial configuration. The next trial proper could not begin until a correct response was made on a correction trial. Mice were given 30 trials (excluding any correction errors) per session (1 session per day) until they attained a performance criterion of >85% correct responses on 2 consecutive session.

The following dependent measures were analyzed: percent correct responding (calculated as the number of correct responses made on the 30 choice trials each session)*100), errors (including correction errors) per session, total responses made, latency to choice, latency to reward, and inter-trial interval. In addition, to examine the microstructure of behavior, the trial-to-trial sequence of choices was determined in order to calculate the average length of strings of consecutive correct and error responses, the percentage of trial pairs in which a correct response was followed by another response at the correct stimulus (= 'win-

stay') and the percentage of trial pairs in which an error was followed by a response at the correct stimulus (= 'lose-shift'). For all measures, learning was segregated into mutually exclusive early, mid and late phases by equally subdividing the number of sessions to criterion for each mouse into the first, second and third groups of sessions (e.g., 9 sessions to criterion = 3 early, 3 mid, 3 late sessions). For session totals indivisible by 3, the additional session(s) accrued to the late, then mid phase. All statistical analyses were corrected for multiple comparisons, using the Benjamini and Hochberg false discovery rate correction (Benjamini and Hochberg, 1995; Bergstrom et al., 2013).

Viral infusion and optical fiber implantation

Mice were placed in a stereotaxic alignment system (Kopf Instruments, Tujunga, CA, USA) to infuse virus and implant ferrules under isoflurane anesthesia. For pathway non-specific DMS and DLS photosilencing, rAAV8/CAG-ArchT-GFP or rAAV8/CAG-GFP (titer: 2×10^{12} molecules/mL, obtained from the UNC Vector Core, Chapel Hill, NC, USA, http://www.med.unc.edu/genetherapy/vectorcore) was bilaterally infused (0.35 µL/hemisphere) over 10 minutes using a Hamilton syringe and 33-gauge needle. The needle was left in place for a further 10 minutes to ensure diffusion. The coordinates for DLS infusions were anteroposterior +1.0 mm, mediolateral ±2.25 mm and dorsoventral -3.1 mm relative to bregma. During the same surgeries, ceramic ferrules were implanted 0.2 mm above the viral injection site to direct optical fibers at the infected region. Ferrules were secured to the skull with jeweler's screws, cyanoacetate and acrylic cement. Each fiber optic ferrule assembly consisted of a 200 µm diameter multimodal fiber (0.39 NA, Thorlabs, Newton, NJ, USA) contained within a 230 µm diameter ceramic ferrule (Precision Fiber Products, South Hillview Milpitas, CA, USA).

All behavioral testing and ex vivo analyses began no earlier than 3 weeks after surgery, to allow for recovery and virus expression. At the completion of testing, to verify accurate ferrule placements mice were deeply anaesthetized with a ketamine (100 mg/kg)/xylazine (10 mg/kg) cocktail then transcardially perfused with phosphate buffered saline, then 4% paraformaldehyde. After suspension in 4% PFA overnight and then 4°C 0.1M phosphate buffer for 1-2 days, 50 µm coronal sections were cut with a vibratome (Leica VT1000 S, Leica Biosystem Inc, Buffalo Grove, IL, USA) and coverslipped with Vectashield HardSet mounting medium and DAPI (Vector Laboratories, Inc., Burlingame, CA, USA). Ferrule location was determined with the aid of an Olympus BX41 microscope (Olympus, Center Valley, PA, USA). Mice without bilateral viral expression or correct ferrule placement were removed from the analysis.

Effects of DLS-silencing on *ex vivo* neuronal activity

DLS slice recordings were conducted based on previously described procedures (Wills et al., 2012). Brain slices (300 µm-thick) containing the dorsal striatum were prepared from C57BL/6J mice at least 5 weeks after bilateral infusion of rAAV8/CAG-ArchT-GFP into the DLS, as described above. Slices were then allowed to recover for 30 minutes in a submerged recording chamber at 32-34°C containing oxygenated sucrose-ACSF (in mM: 208 sucrose, 2.5 KCl, 1.6 NaH_2PO_4, 1 $CaCl_2{\cdot}2H_2O$, 4 $MgCl_2{\cdot}6H_2O$, 4 $MgSO_4{\cdot}7H_2O$, 26 $NaHCO_3$, 1 ascorbate, 3 Na-pyruvate, and 20 glucose). Following this recovery period, the slices were maintained in heated (28˚C), oxygenated (95% O2–5% CO2) 'normal' ACSF (in mM: 124 NaCl, 4.4 KCl, 2 CaCl2, 1.2 MgSO4, 1 NaH2PO4, 10.0 glucose, and 26.0 NaHCO3, pH 7.2–7.4; 290–310 mOsm) for at least 1 hour before being transferred to submerged perfusion chamber (also heated to 27–30°C) for whole-cell, current-clamp recordings. All electrophysiology recordings were made using Clampex 9.2 and analyzed using Clampfit 10.2 (Molecular Devices, Sunnyvale, CA, USA). Whole-cell, current-clamp recordings were performed in neurons within the area of viral infection (identified by GFP) and carried out at each neuron's resting membrane potential after allowing at least 3 minutes for the cell to equilibrate and for the resting membrane potential to stabilize. Recording electrodes for current-clamp experiments were filled with (in mM): 135 K+-gluconate, 5 NaCl, 2 MgCl2, 10 HEPES, 0.6 EGTA, 4 ATP, 0.4 GTP, pH 7.2–7.3, 280–290 mOsmol. Current injections (0.5 Hz/1500 milliseconds) were given in 20 pA steps until the cell reached threshold and fired a single AP. Approximately 10 additional current injections steps (20 pA each) were given above threshold. Light generated by X-Cite (Series 120, Excelitas Technologies Waltham, MA, USA) through YFP filter cube produced full-field illumination for the

duration of current injection. Light activation occurred at every third current injection at which time AP firing rate had typically returned to pre-light levels.

Effects of DLS-silencing in the open field and real-time place preference (RTPP) tests

Mice were bilaterally infected with either rAAV8/CAG-ArchT-GFP or rAAV8/CAG-GFP and tested in the open field, using previously described methods (Karlsson et al., 2008; Kravitz et al., 2010). Mice were placed in the center of a white Plexiglas arena (40 x 40 x 30 cm), lit to ~100 lux, for a 15-minute test. Laser was turned on (illumination parameters as above) for a total of 22 x 10-second periods, each interspersed with 30-second no-laser interval. Distance traveled, movement velocity, movement bouts, and freezing bouts were measured using the EthoVision XT video-tracking system (Noldus Information Technology, Leesburg, VA, USA) using the Lowess Smoothing Method algorithm, as previously described (Kravitz et al., 2012).

At least 1 week after the open field, mice were tested in the RTPP test was previously described methods (Kravitz et al., 2012; Namburi et al., 2015). A white Plexiglas arena (40 x 40 x 30 cm, illuminated to ~100 lux) was subdivided into 2 equally-sized compartments. The mouse began a 20-minute session in the compartment designated as 'unstimulated' (counterbalanced across mice). On each entry into the other compartment, designated 'stimulated,' laser was set to a 10-second ON followed by 10-second OFF period (illumination parameters as above), until the mouse returned to the unstimulated compartment. Distance moved in each compartment was measured using the EthoVision XT video-tracking system, as described above.

Effects of DLS-silencing at choice on learning

Mice were pre-trained (i.e., to pre-training criterion, but without discrimination testing) as described above and then the DLS was bilaterally infected with either rAAV8/CAG-ArchT-GFP or rAAV8/CAG-GFP to silence the DLS during discrimination training. For silencing, light was delivered at trial initiation (head entry into magazine) through choice to reward collection for each correct trial, and at trial initiation through choice to 3 seconds post-choice for each incorrect trial. This 3-second period was chosen *a priori* to approximate the light-on duration for correct trials: the average light-on duration for correct trials was 9.96±0.43 seconds, and 7.93±0.47 seconds for incorrect trials). Rebound activity has been reported in ArchT-infected cultured rat hippocampal neurons, but this effect emerges at longer (~30-seconds) periods of illumination (Mahn et al., 2016) than used here. Moreover, prior studies using ArchT in mice to silence dorsal striatal medium spiny neurons for 5-seconds (Tecuapetla et al., 2016) and hippocampal-cortical neurons for 120-seconds (Padilla-Coreano et al., 2016) did not report evidence of rebound activity from *in vivo* neuronal recordings. Therefore, though we cannot fully exclude the potential for rebound activity in the current study, this seems be an unlikely confound.

Green light was delivered through 65.5 μm bifurcated patch cable (Fiber Optics For Sale Co, Fremont, CA, USA) coupled to a 200-mW, 532-nm, laser system (Opto Engine, Midvale, UT, USA) interfaced with the touchscreen software to deliver TTL pulses to a laser driver. Laser power at the tip of the fiber was measured before each test session using a power meter (PM20, Thorlabs, Newton, NJ, USA) and adjusted to achieve 7 mW (to reduce the potential for heating brain tissue in the vicinity of the tip that can occur at higher power (Christie et al., 2013)). The estimated irradiance at 0.5 mm from the fiber tip was 4.87 mW/mm^2 based on 7 mW at the fiber tip, N.A. 0.37 and 561 nm wavelength light (http://www.stanford.edu/group/dlab/cgi-bin/graph/chart.php) (**Figure 1h**).

Effects of DLS-silencing at reward

A cohort of experimentally naïve C57BL/6J mice were pre-trained on the touchscreen and then bilaterally infected with either rAAV8/CAG-ArchT-GFP or rAAV8/CAG-GFP to silence the DLS. The procedure was the same as described above, with the exception that light was delivered at reward collection: i.e., for 3 seconds following head entry into the magazine after a correct choice.

Effects of DLS-silencing at choice on early learning, with the alternate stimulus rewarded

A cohort of experimentally naïve C57BL/6J mice were pre-trained on the touchscreen and then bilaterally infected with either rAAV8/CAG-ArchT-GFP or rAAV8/CAG-GFP to silence the DLS. The procedure was the same as described above for the silencing at choice experiment, with the exception that the responses at the 'marble' stimulus produced a food reward at a continuous rate of reinforcement, whereas responses at the 'fan' stimulus (='errors') produced no food reward and a 15-second 'timeout' period. Mice were tested on the first 3 sessions of discrimination training, corresponding to the early learning stage.

Effects of DLS-silencing at choice on learning criterion

A cohort of experimentally naïve C57BL/6J mice were pre-trained on the touchscreen and then bilaterally infected with either rAAV8/CAG-ArchT-GFP or rAAV8/CAG-GFP to silence the DLS. The procedure was the same as described above, with the exception that silencing was restricted to the 3 sessions after a mouse had been given discrimination training, without silencing, to attain at least 85% correct performance on two consecutive test days. This corresponded to silencing during the late learning stage.

Effects of DLS-silencing on learning on spatiotemporal measures

A cohort of experimentally naïve C57BL/6J mice were pre-trained on the touchscreen and then bilaterally infected with either rAAV8/CAG-ArchT-GFP or rAAV8/CAG-GFP to silence the DLS during choice, as described above. Behavior was recorded on sessions corresponding to the early, mid and late stages (as defined above) using a Lafayette Instruments overhead infrared video camera. Videos were then analyzed offline, using EthoVision XT v.11 software (Noldus Information Technology, Leesburg, VA, USA) using the Lowess Smoothing Method algorithm, as previously described (Kravitz et al., 2012). The apparatus was segregated into 3 zones: a 24 x 5 cm area adjacent to the touchscreen, a 10 x 5 cm area adjacent to the magazine and a 15 x 7 cm 'runway' occupying the area between the touchscreen and magazine zones. Session duration, inter-trial interval, number of zone visits, movement speed, and distance moved in each zone was measured.

Assessment of learning-related DLS output-pathway recruitment

A cohort of experimentally naïve C57BL/6J mice were pre-trained and then 1 group was given 2 discrimination sessions (= early group), and the other group was trained to criterion (= late group). Fifteen minutes after the final test session, mice were sacrificed using cervical dislocation and brains frozen in 2-methyl butane on dry ice prior to processing for fluorescence *in situ* hybridization, as described below. Here, the target probes were Mm-*Arc* (gene ID 11838, Cat# 316911-C2), Mm-*Drd1* (gene ID 13488, Cat #406491-C1) and Mm-*Drd2* (gene ID: 13489, Cat# 406501-C3).

Brains were placed in a cryostat (HM500 OM, Microm International GmbH, Walldorf, Germany) chamber to equilibrate for 2 hours at -20°C. 16-µm sections containing the DLS were collected and mounted directly onto Super Frost Plus slides (Fisher Scientific, Pittsburgh, PA, USA) and kept at -20°C before being transferred to a slide rack in a staining jar of 10% buffered formalin solution pre-chilled to 4°C for fixation, according to the manufacturer's protocol. After fixation for 20 minutes, the slides were rinsed twice in PBS for one minute each, and then were dehydrated in an ethanol dilution series (50%, 70%, 100% x2). The fixed slides were stored in fresh 100% ethanol overnight at -20°C.

The following day, the slides were air dried for 10 minutes and a hydrophobic barrier was drawn around each section with an Immedge™ barrier pen to limit the spread of solutions. Samples were pretreated with Pretreat-4 protease solution for 20 minutes at room temperature, and the slides were washed twice with distilled water. Target probes were then applied to the sections, spread evenly with a pipette tip, and the slides were incubated at 40°C for 2 hours in an oven (HybEZ, Advanced Cell Diagnostics Hayward, CA, USA). Sections were then treated with amplifier and fluorescently labeled probes (AMP1 at 40°C for 30 minutes; AMP2 at 40°C for 15 minutes; AMP3 at 40°C for 30 minutes; AMP4 AltC at 40°C for 15 minutes). Slides were washed twice with 1X wash buffer between incubation steps. Finally, the sections were incubated for 20 seconds with DAPI, and then coverslipped with Vectashield fluorescent mounting medium

(H-1400; Vector Laboratories, Burlingame, CA, USA). Positive control (3 probe sets to a house-keeping gene) and negative control (3 probe sets for bacterial mRNA) treated sections were included for each brain.

Fluorescent images (2 sections per brain, 3 images per hemisphere) of the DLS were taken with a Zeiss (LSM 700, Carl Zeiss Microscopy, Thornwood, NY, USA) confocal microscope under a Plan-Apochromat 20x/0.8 M27 objective. The images were separated by fluorescent channel for individual relative quantification using Zen lite digital imaging software (Zeiss). Three 320 μm^2 regions were imaged per hemisphere, using the corpus callosum as an anatomical reference point to maintain consistency between sections/animals. DAPI-stained neurons were marked with a circle drawn around the soma using ImageJ. On the fluorescent channel corresponding to *Arc*, the number of pixels within each neuron's somatic area was calculated to determine the average number of *Arc*-positive cells per ROI. Of these *Arc*-labelled cells, the number that were also *Drd1*- or *Drd2*-labeled (via calculation of ImageJ generated pixel counts on the corresponding fluorescent channels), or labeled with neither probe, was determined to calculate the % of *Arc*/*Drd1* and *Arc*/*Drd2* (or neither) cells. Overall there were 3 mice/1800 D1 and D2 cells/707 Arc-expressing cells in the early group and 3 mice/2,040 D1 and D2 cells/655 Arc-expressing in the late group. All counts were conducted blind to experimental group.

Comparison of induced Arc expression in the DLS direct and indirect pathways

Hemizygous *B6.Cg-Tg(Drd1a-tdTomato)6Calak/J* (JAX stock # 016204) x hemizygous *Tg(Drd2-EGFP)S118Gsat* (GENSAT) dual-reporter mice (backcrossed onto a C57BL/6J background for an undetermined number of generations) (Ade et al., 2011) were intraperitoneally injected with 60-70 mg/kg (in a saline vehicle at a volume of 10 mL/kg body weight) of the seizure-inducing compound, pentylenetetrazole (Kee et al., 2007). One hour later, mice were deeply anaesthetized with a ketamine/xylazine cocktail and transcardially perfused with 4% paraformaldehyde, the brain removed and post-fixed overnight in 4% paraformaldehyde. Fifty-µm coronal sections were cut on a vibratome (Leica VT1000 S, Leica Biosystem Inc, Buffalo Grove, IL, USA). Sections were washed in PBS, blocked with 1% BSA, 10% Normal Goat Serum, 0.3% Triton-X 100 in PBS for 2 hours at room temperature, then incubated overnight at 4ºC with either mouse monoclonal anti-Arc (cat#: sc-17839, 1:50, C-7, Santa Cruz Biotechnology, Santa Cruz, CA, USA) or anti-Arc (SYnaptic SYstems, Goettingham, Germany), followed by incubation for 2 hours at room temperature with either AlexaFluor 680 (Abcam, Cambridge, UK) or AlexaFluor 647 (Life Technologies, Carlsbad, CA, USA), respectively. After the reaction, serial sections containing the DLS were counterstained with 5 µg/mL Hoechst 33342 (Life Technologies) and were mounted onto slides, air-dried and then coverslipped with aqueous mounting media.

Fluorescent images (6 sections per brain, 3 images per hemisphere) of the DLS were taken with a Zeiss (LSM 710, Carl Zeiss Microscopy, Thornwood, NY, USA) confocal microscope under a Plan-Apochromat 20x/0.8 M27 objective (1.8 µm optical section). The images (640 μm^2) were separated by fluorescent channel for individual relative quantification using Fiji (Schindelin et al., 2012). A 320 μm^2 region of interest (ROI) was set in each image and all *Drd1*-labeled and *Drd2*-labeled cells were marked with a circle using a custom-written Fiji macro (using the Clear All command to limit the analysis to within the ROI, background correction with CLAHE, autothreshold with MaxEntropy command and new neuronal ROIs around the cell's somatic area using the Analyze particle command). The neuronal ROIs were applied on the fluorescent channel corresponding to Arc and the cumulative Arc intensity on either *Drd1* or *Drd2* cells was calculated and compared between pentylenetetrazole-injected mice and controls sacrificed immediately after removal from the home cage. The percentage of colocalized Arc/*Drd1* and Arc/*Drd2* cells was also calculated by defining a cell as Arc-labeled if the average intensity exceeded a threshold at which the maximal average intensity differed between the experimental groups.

Effects of DLS direct-pathway silencing on learning

Male *Drd1*-Cre-positive mutants obtained from The Mutant Mouse Regional Resource Centers (stock #030779-UCD, C57BL/6J background) (Gerfen et al., 2013) were mated with C57BL/6J females to produce Cre-positive and Cre-negative littermates for testing. Following pre-training, the DLS was

bilaterally infected with rAAV5/EF1a-DIO-eArch3.0-eYFP (titer: 3.2 x 10-12 molecules/mL, UNC Vector Core) and optical fibers implanted, as above. Green light was shone during choice, as described above.

Effects of DLS indirect-pathway silencing on learning

Male *Adora2a*-Cre-positive mutants obtained from The Mutant Mouse Regional Resource Centers (stock #KG139, C57BL/6J background) (Gerfen et al., 2013) were mated with C57BL/6J females to produce Cre-positive and Cre-negative littermates in which the DLS was silenced during choice, as described above.

Assessment of system-level adaptations due to DLS-silencing

A cohort of experimentally naïve C57BL/6J mice were pre-trained on the touchscreen and then bilaterally infected with either rAAV8/CAG-ArchT-GFP or rAAV8/CAG-GFP to silence the DLS. The DLS was silenced during choice, as described above. One group was given 2 discrimination sessions (= early group), and another group was trained to criterion (= late group). One hour after testing, mice were deeply anaesthetized with a ketamine/xylazine cocktail then transcardially perfused with ice cold phosphate buffered saline (PBS, pH 7.4) followed by ice cold 4% paraformaldehyde. The number of total trials made on the session before sacrifice did not significantly differ between the groups (Early: GFP=141±8 versus ArchT=134±19 trials, Late: GFP=173±17 versus ArchT=134±12 trials). Brains were removed and 35-µm coronal sections cut on a vibratome (Leica VT1000 S, Leica Biosystem Inc, Buffalo Grove, IL, USA) and stored free floating in PB 0.1M at 4° C for no longer than 1 week.

Sections were first thoroughly rinsed 3X for 10 minutes in PBS. To reduce background peroxidase activity, sections were then incubated in 50% ethanol in PBS 3X for 15 minutes and then incubated in 1% hydrogen peroxide in 50% ethanol/PBS for 15 minutes. Next, the sections were washed 3X for 10 minutes in PBS and blocked in 5% normal goat serum and 3% bovine serum albumin in PBS-TritonX (0.3%) for 30 minutes. Sections were incubated overnight in mouse monoclonal anti-Arc (cat#: sc-17839, 1:50, C-7, Santa Cruz Biotechnology, Santa Cruz, CA, USA) in a dilution of 0.3% TritonX, 0.5% normal goat serum in PBS on a platform rocker at room temperature. Sections were then rinsed 3X for 10 minutes in PBS and incubated in anti-mouse secondary antibody (cat#: BA9200, 1:1000, Vector Labs, Burlingame, CA, USA) in 0.3% TritonX, 0.1% normal goat serum for 90 minutes. Sections were rinsed in PBS 3X for 10 minutes and then incubated in avidin-biotin complex solution for 45 minutes. Sections were again rinsed in PBS then TRIS-HCl buffer (pH 7.2) 2X for 10 minutes. Next, sections were incubated in a diaminobenzidine-hydrogen peroxide reaction for 3 minutes. After the reaction, sections were rinsed 2X for 10 minutes in TRIS-HCl buffer and then rinsed in PB 0.1 M for 10 minutes. Serial sections were mounted onto gelatinized slides, air-dried, then dehydrated in a graded series of alcohol then xylene, and coverslipped with permount.

Arc-positive cells that were clearly distinguishable from background staining were manually counted under a 20X/0.5 N.A. objective in a 0.25 mm^2 counting frame using Neurolucida v11 (MBF Biosciences, Williston, VT, USA) interfaced with a bright field microscope (Olympus BX-40, Olympus, Center Valley, PA, USA) and digital camera. For all bright field microscopy, Koehler illumination principles were applied. A total of 8 cortical and striatal brain regions were identified, with the help of major anatomical landmarks illustrated in a standard mouse brain atlas (Paxinos and Franklin, 2004): agranular insular cortex (from AP = +2.30, ML = ± 2.25, DV = -3.0 to AP = +2.0, ML = ± 2.75, DV = −3.5), prelimbic cortex (from AP = +2.0, ML = ± 0.25, DV = 2.0 to AP = +1.54, ML = ± 0.25, DV = −2.25), somatosensory cortex (from AP = +1.54 , ML = ± 2.85, DV = -2.50 to AP = +0.14, ML = ±3.25, DV = -2.0), dorsomedial striatum (from AP = +1.10, ML = ± 0.80, DV = −3.00 to AP = +0.26, ML = ±1.25, DV = -2.75), nucleus accumbens core (from AP = +1.78, ML = ± 0.75, DV = −4.50 to AP = +0.98, ML = ± 1.0, DV = −4.75), nucleus accumbens shell (from AP = +1.78, ML = ± 0.75, DV = −4.50 to AP = +0.86, ML = ± 0.5, DV = -5.0), basolateral nucleus of the amygdala (from AP = -0.94, ML = ±2.75, DV = -4.75 to AP = -1.70, ML = ±3.0, DV = -4.75), and the central nucleus of the amygdala (from AP = -0.94, ML = ±2.25, DV = -4.75 to AP = -1.58, ML = ±2.5, DV = -4.5). Counts in the globus pallidus interior, globus pallidus exterior and substantia nigra reticulata were not made due to weak and diffuse Arc staining in these regions. For each brain region, cell counts were conducted (blind to experimental condition) in 3 sections from each hemisphere, for a total of

6 data points per region per mouse. It was unnecessary to correct for double counting because sections were non-consecutive. Only mice with confirmed optical fibers and viral expression located in the DLS were included in the analysis. Counts are presented as the mean number of Arc-positive cells per 0.25 mm^2.

Effects of DMS-silencing at choice on learning

A cohort of experimentally naïve C57BL/6J mice were pre-trained on the touchscreen and then bilaterally infected with either rAAV8/CAG-ArchT-GFP or rAAV8/CAG-GFP and had optical fibers implanted into the DMS (coordinates: anteroposterior +0.50 mm, mediolateral ±1.50 mm and dorsoventral -2.50 mm relative to bregma). Green light was shone during choice, as described above.

Effects of DMS-silencing at choice on mid stage learning

A cohort of experimentally naïve C57BL/6J mice were pre-trained on the touchscreen and then bilaterally infected with either rAAV8/CAG-ArchT-GFP or rAAV8/CAG-GFP to silence the DMS. The procedure was the same as described above, with the exception that silencing was restricted to the 3 sessions after a mouse had been given discrimination training, without silencing, to attain at least 60% correct performance (which required an average 4.6 sessions across the cohort). This corresponded to silencing during the mid-learning stage.

References

Ade KK, Wan Y, Chen M, Gloss B and Calakos N (2011) An Improved BAC Transgenic Fluorescent Reporter Line for Sensitive and Specific Identification of Striatonigral Medium Spiny Neurons. *Frontiers in Systems Neuroscience* 5: 32.

Benjamini Y and Hochberg Y (1995) Controlling the false discovery rate: a practical and powerful approach to multiple testing. *Journal of the Royal Statistical Society.Series B (Methodological)*: 289-300.

Bergstrom HC, McDonald CG, Dey S, Fernandez GM and Johnson LR (2013) Neurons activated during fear memory consolidation and reconsolidation are mapped to a common and new topography in the lateral amygdala. *Brain Topography* 26(3): 468-478.

Brigman JL, Daut RA, Wright T, Gunduz-Cinar O, Graybeal C, Davis MI, et al. (2013) GluN2B in corticostriatal circuits governs choice learning and choice shifting. *Nature Neuroscience* 16(8): 1101-1110.

Christie IN, Wells JA, Southern P, Marina N, Kasparov S, Gourine AV, et al. (2013) fMRI response to blue light delivery in the naive brain: implications for combined optogenetic fMRI studies. *NeuroImage* 66: 634-641.

Gerfen CR, Paletzki R and Heintz N (2013) GENSAT BAC cre-recombinase driver lines to study the functional organization of cerebral cortical and basal ganglia circuits. *Neuron* 80(6): 1368-1383.

Graybeal C, Feyder M, Schulman E, Saksida LM, Bussey TJ, Brigman JL, et al. (2011) Paradoxical reversal learning enhancement by stress or prefrontal cortical damage: rescue with BDNF. *Nature Neuroscience* 14(12): 1507-1509.

Horner AE, Heath CJ, Hvoslef-Eide M, Kent BA, Kim CH, Nilsson SR, et al. (2013) The touchscreen operant platform for testing learning and memory in rats and mice. *Nature Protocols* 8(10): 1961-1984.

Izquierdo A, Wiedholz LM, Millstein RA, Yang RJ, Bussey TJ, Saksida LM, et al. (2006) Genetic and dopaminergic modulation of reversal learning in a touchscreen-based operant procedure for mice. *Behavioural Brain Research* 171(2): 181-188.

Karlsson R, Tanaka K, Heilig M and Holmes A (2008) Loss of glial glutamate and aspartate transporter (excitatory amino acid transporter 1) causes locomotor hyperactivity and exaggerated responses to psychotomimetics: rescue by haloperidol and metabotropic glutamate 2/3 agonist. *Biological Psychiatry* 64(9): 810-814.

Kee N, Teixeira CM, Wang AH and Frankland PW (2007) Imaging activation of adult-generated granule cells in spatial memory. *Nature Protocols* 2(12): 3033.

Kravitz AV, Tye LD and Kreitzer AC (2012) Distinct roles for direct and indirect pathway striatal neurons in reinforcement. *Nature Neuroscience* 15(6): 816-818.

Kravitz AV, Freeze BS, Parker PR, Kay K, Thwin MT, Deisseroth K, et al. (2010) Regulation of parkinsonian motor behaviours by optogenetic control of basal ganglia circuitry. *Nature* 466(7306): 622-626.

Mahn M, Prigge M, Ron S, Levy R and Yizhar O (2016) Biophysical constraints of optogenetic inhibition at presynaptic terminals. *Nature Neuroscience* 19(4): 554-556.

Namburi P, Beyeler A, Yorozu S, Calhoon GG, Halbert SA, Wichmann R, et al. (2015) A circuit mechanism for differentiating positive and negative associations. *Nature* 520(7549): 675-678.

Padilla-Coreano N, Bolkan SS, Pierce GM, Blackman DR, Hardin WD, Garcia-Garcia AL, et al. (2016) Direct ventral hippocampal-prefrontal input is required for anxiety-related neural activity and behavior. *Neuron* 89(4): 857-866.

Paxinos G and Franklin KB (2004) *The Mouse Brain in Stereotaxic Coordinates.* : Elsevier.

Schindelin J, Arganda-Carreras I, Frise E, Kaynig V, Longair M, Pietzsch T, et al. (2012) Fiji: an open-source platform for biological-image analysis. *Nature Methods* 9(7): 676-682.

Tecuapetla F, Jin X, Lima SQ and Costa RM (2016) Complementary contributions of striatal projection pathways to action initiation and execution. *Cell* 166(3): 703-715.

Wills TA, Klug JR, Silberman Y, Baucum AJ, Weitlauf C, Colbran RJ, et al. (2012) GluN2B subunit deletion reveals key role in acute and chronic ethanol sensitivity of glutamate synapses in bed nucleus of the stria terminalis. *Proceedings of the National Academy of Sciences of the United States of America* 109(5): E278-87.

a
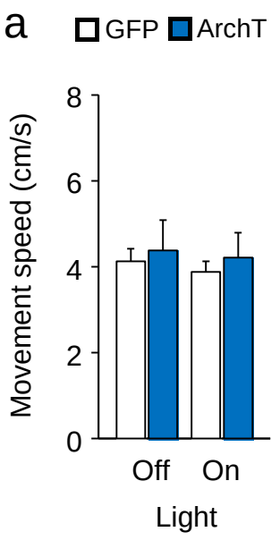

b
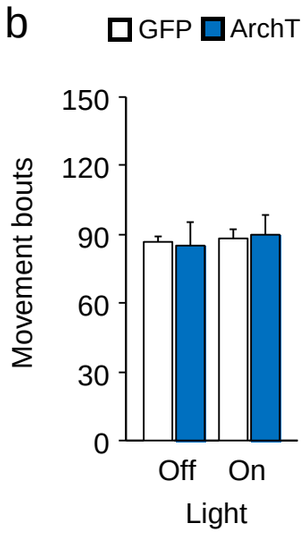

c
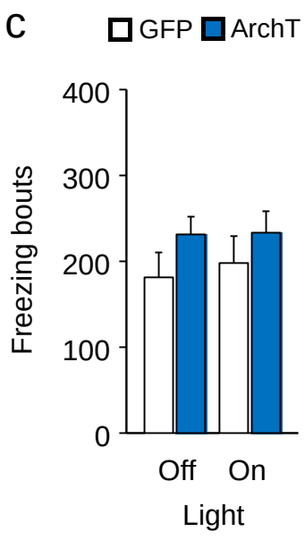

d
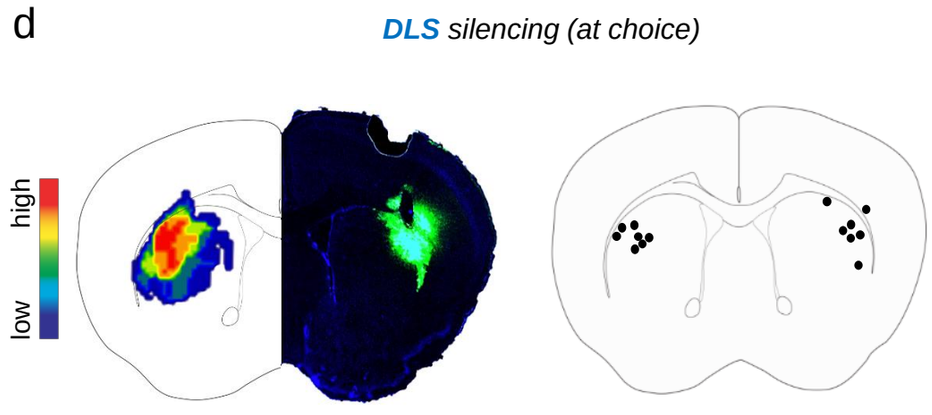

e
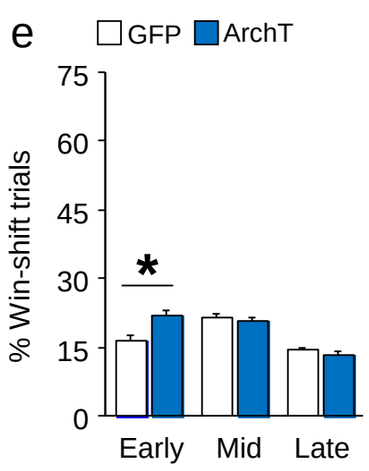

f
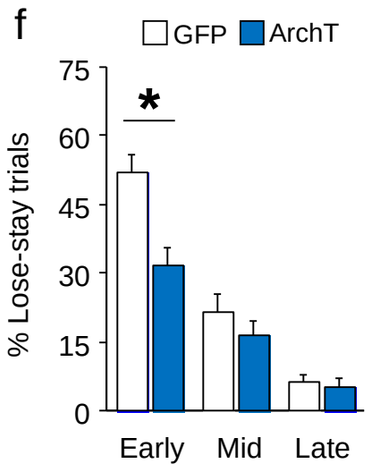

g
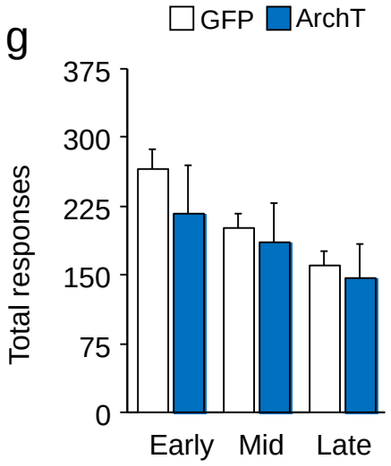

h
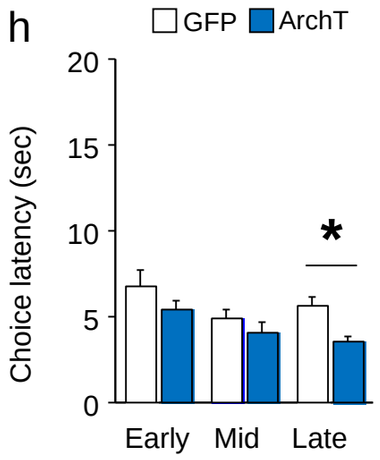

i
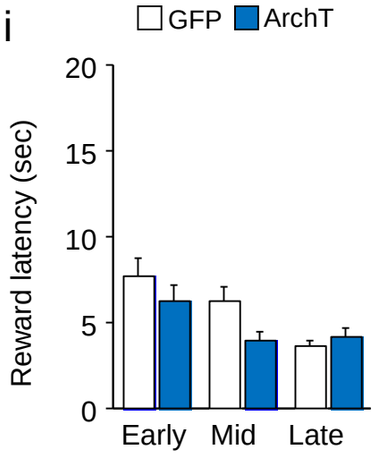

j
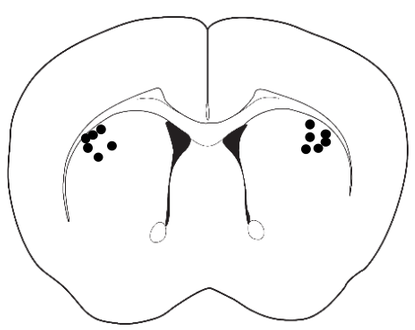

k
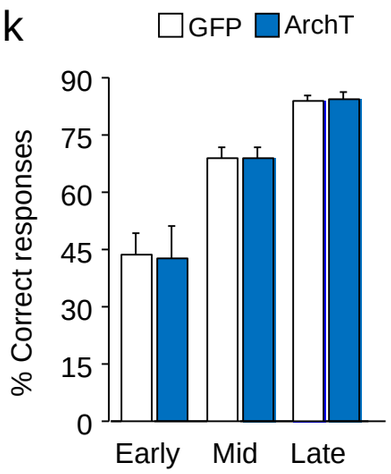

l
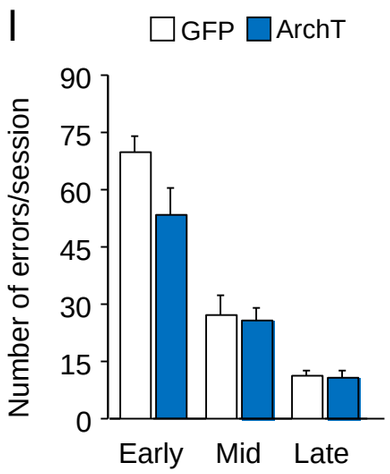

m
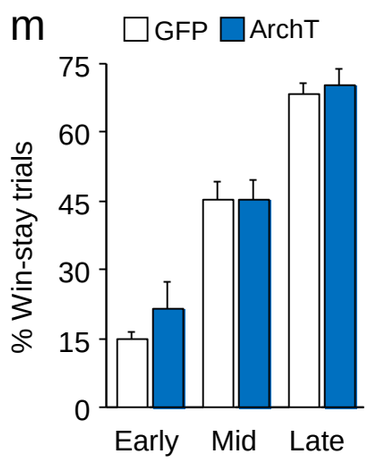

n
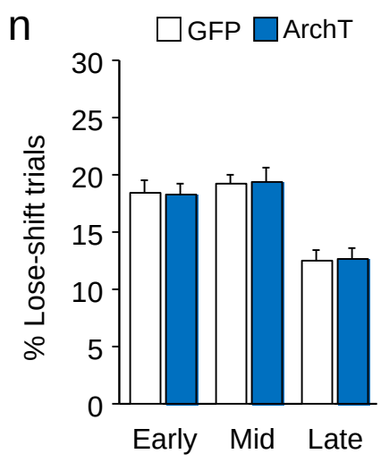

o
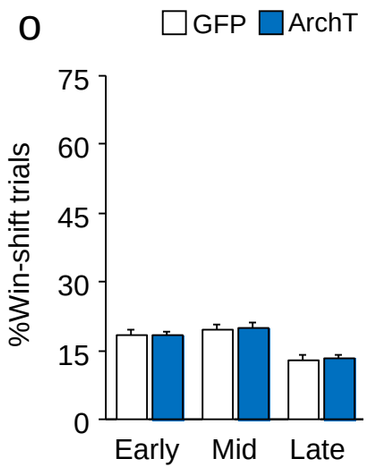

p
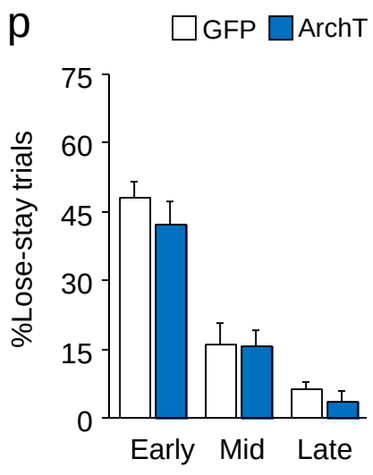

q
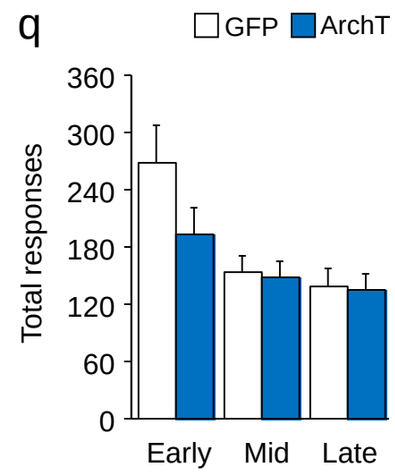

r
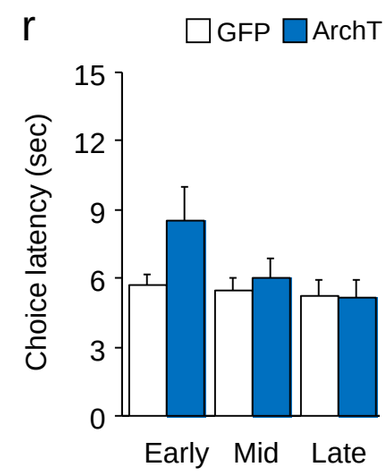

s
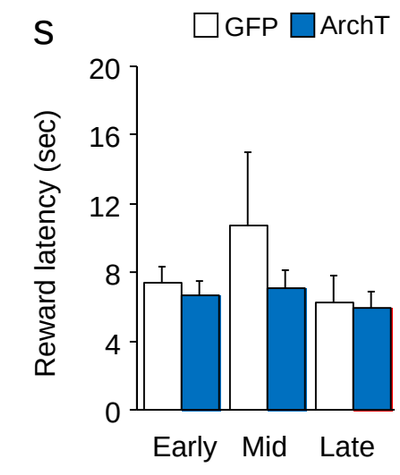

Figure S1: Effects of DLS-photosilencing on open field motoric behaviors, real-time place-preference, auxiliary touchscreen-task measures, and reward. Related to Figure 1 and 2. Movement speed (**a**) movements bouts (**b**) and freezing bouts (**c**) did not differ between GFP and ArchT groups on either (10-second) light-on and (30-second) light-off periods during a 15-minute test (group x light ANOVA: $P>.05$). Example of virus localization and estimates of optical fiber placements (**d**). The ArchT group had increased %win-shift trials ($t(14)=3.00$, $P<0.01$) (**e**) and decreased %lose-stay trials ($t(14)=3.41$, $P<0.01$) (**f**), as compared to the GFP group at early-learning. Total responses made did not differ between GFP and ArchT groups (**g**). The ArchT group had faster choice latency than the GFP group at late-learning ($t(14)=2.76$, $P<0.01$) (**h**). Latency to collect reward did not differ between GFP and ArchT groups (**i**). Estimates of optical fiber placements in the photosilencing at reward experiment (**j**). Percent correct responses did not differ between GFP and ArchT groups (**k**). Errors-rates did not differ between GFP and ArchT groups (**l**). Win-stay (**m**), lose-shift (**n**), win-shift (**o**) and lose-stay (**p**) behavior did not differ between GFP and ArchT groups. Total responses did not differ between GFP and ArchT groups (**q**). Choice latency did not differ between GFP and ArchT groups (**r**). Latency to collect reward did not differ between GFP and ArchT groups (**s**). *$P<.05$. Data are mean±SEM.

a

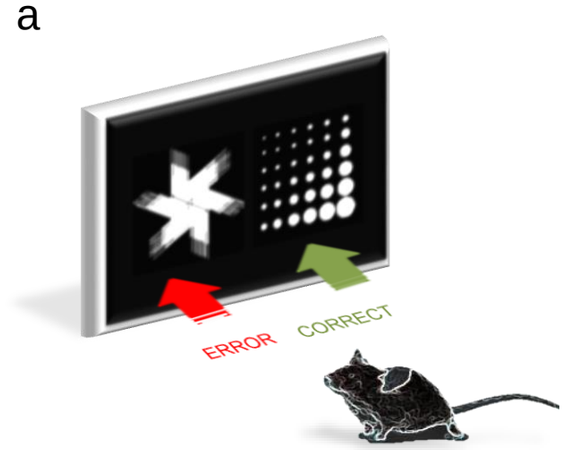

b

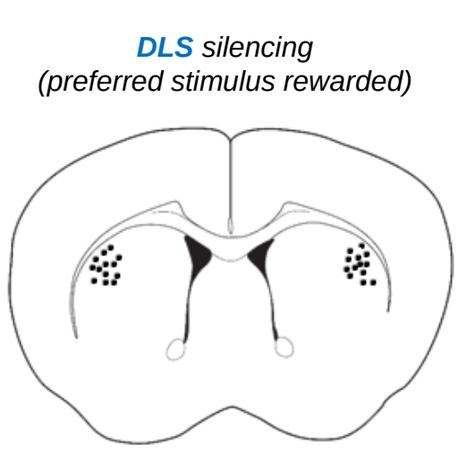

c

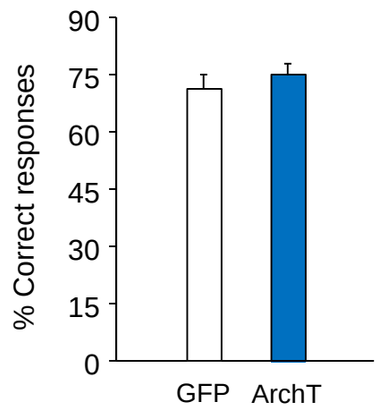

d

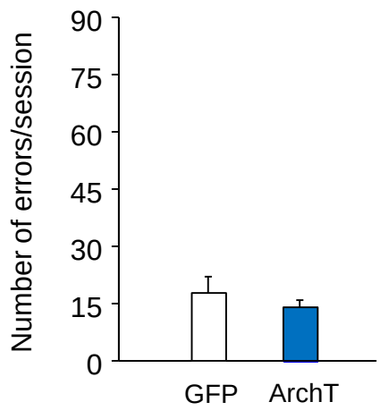

e

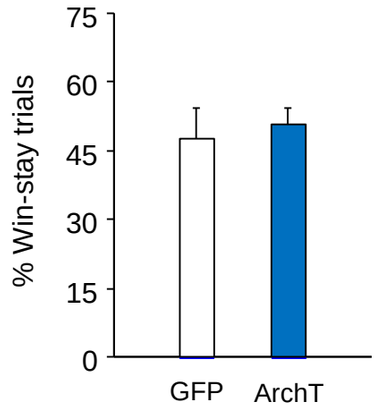

f

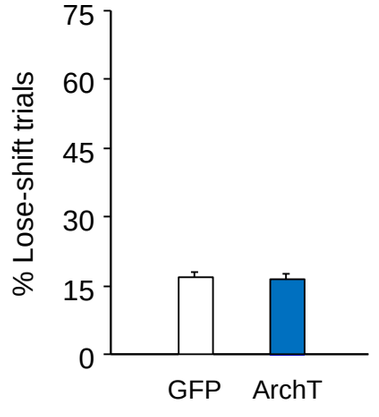

g

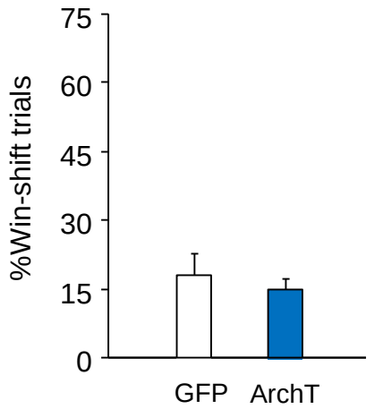

h

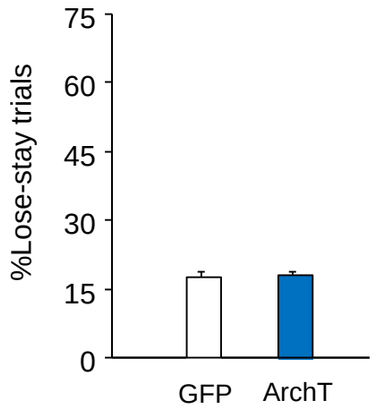

i

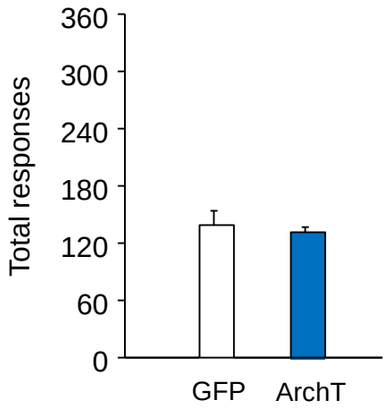

j

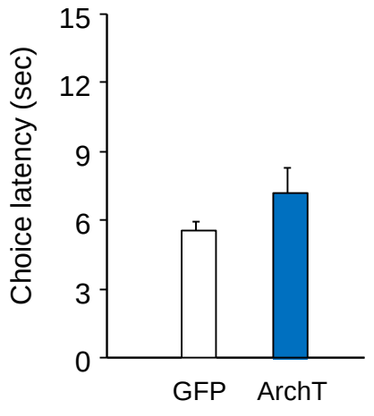

k

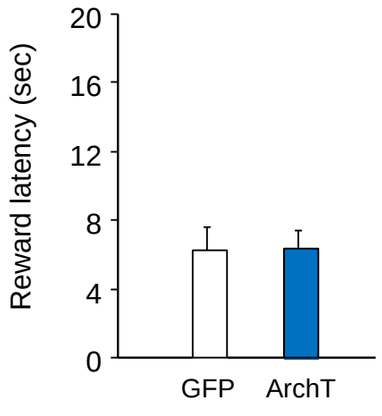

l

DLS silencing
(performance at criterion)

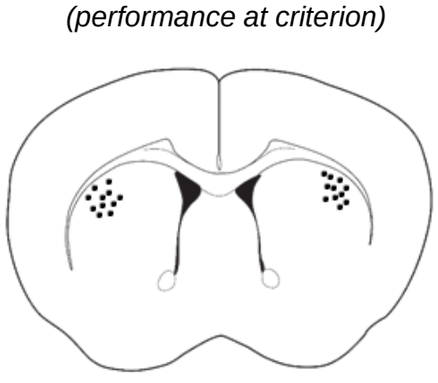

m

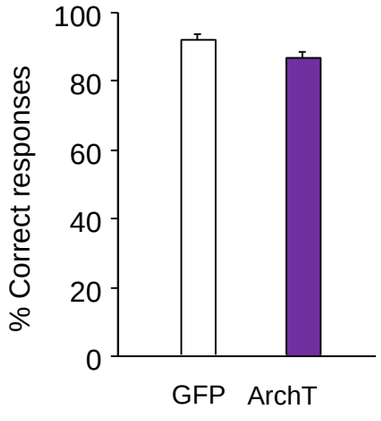

n

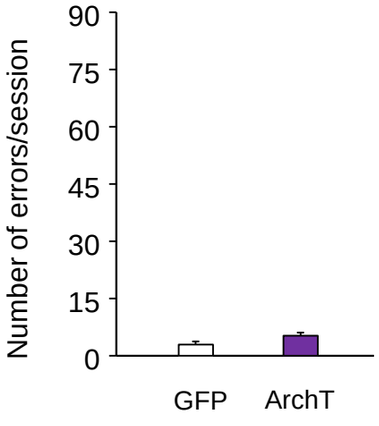

o

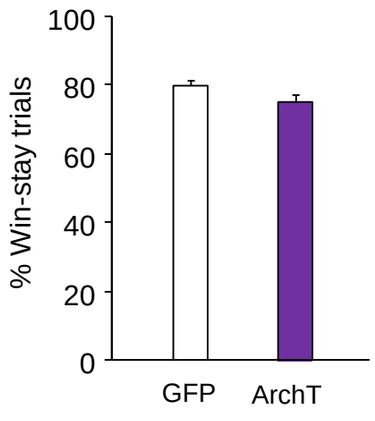

p

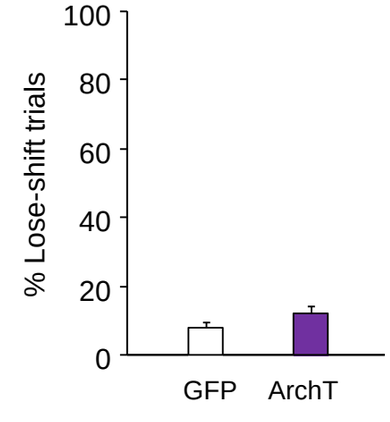

q

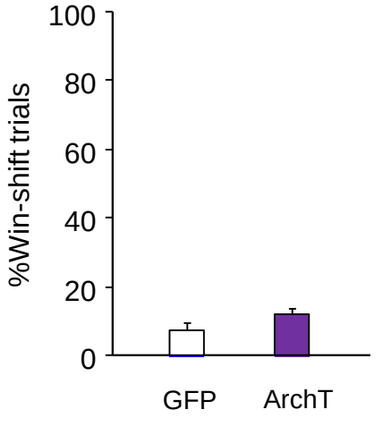

r

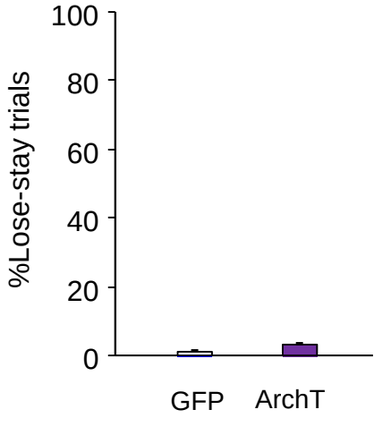

s

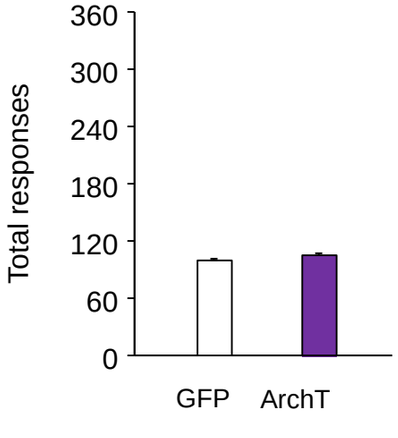

t

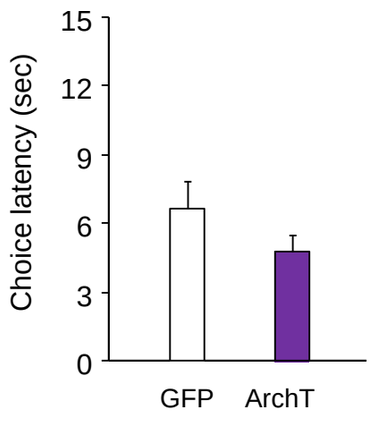

u

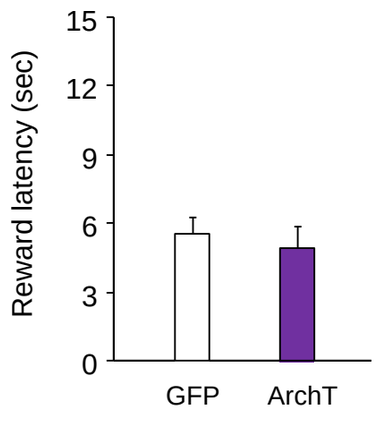

Figure S2: Effects of early learning DLS-photosilencing at choice, with the visually preferred stimulus rewarded, and beginning after criterion performance attained. Related to Figure 1 and 2. Touchscreen visual discrimination training with the preferred, 'fan,' stimulus rewarded (**a**). Estimates of optical fiber placements in the photosilencing at reward experiment (**b**). Percent correct responses did not differ between GFP and ArchT groups (n=5-8) (**c**). Errors-rates did not differ between GFP and ArchT groups (**d**). Win-stay (**e**), lose-shift (**f**), win-shift (**g**), and lose-stay (**h**) behavior did not differ between GFP and ArchT groups. Total responses did not differ between GFP and ArchT groups (**i**). Choice latency did not differ between GFP and ArchT groups (**j**). Latency to collect reward did not differ between GFP and ArchT groups (**k**). Estimates of optical fiber placements in the photosilencing at reward experiment (**l**). Percent correct responses did not differ between GFP and ArchT groups (n=5-8) (**m**). Errors-rates did not differ between GFP and ArchT groups (**n**). Win-stay (**o**), lose-shift (**p**), win-shift (**q**), and lose-stay (**r**) behavior did not differ between GFP and ArchT groups. Total responses did not differ between GFP and ArchT groups (**s**). Choice latency did not differ between GFP and ArchT groups (**t**). Latency to collect reward did not differ between GFP and ArchT groups (**u**). **P*<.05. Data are mean±SEM.

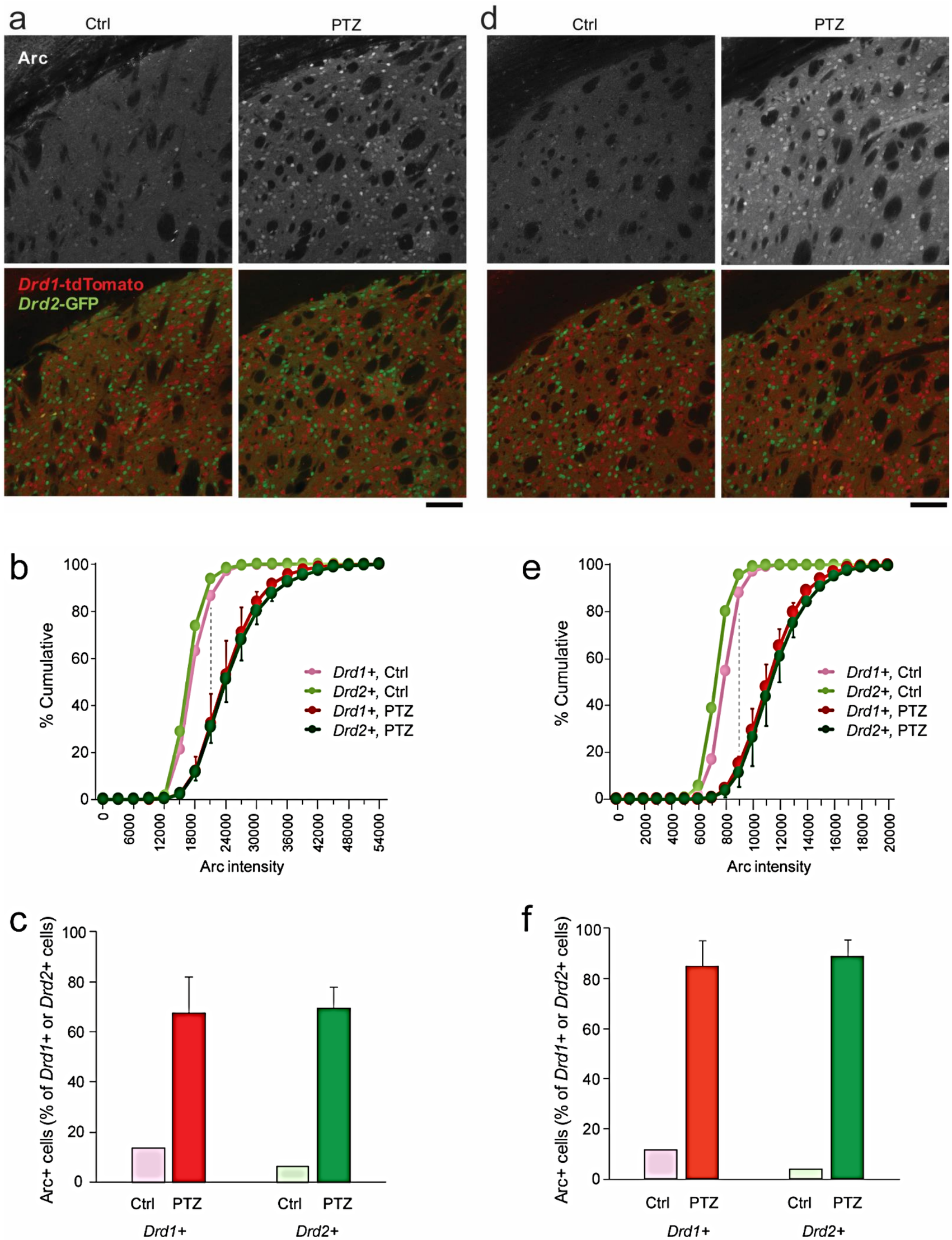
a
Ctrl
PTZ
Arc
Drd1-tdTomato
Drd2-GFP
d
Ctrl
PTZ
b
% Cumulative
Drd1+, Ctrl
Drd2+, Ctrl
Drd1+, PTZ
Drd2+, PTZ
Arc intensity
e
% Cumulative
Drd1+, Ctrl
Drd2+, Ctrl
Drd1+, PTZ
Drd2+, PTZ
Arc intensity
c
Arc+ cells (% of Drd1+ or Drd2+ cells)
Ctrl
PTZ
Drd1+
Drd2+
f
Arc+ cells (% of Drd1+ or Drd2+ cells)
Ctrl
PTZ
Drd1+
Drd2+

Figure S3: Comparison of induced *Arc* expression in the direct and indirect DLS output pathways. Related to Figure 3. Representative images of Arc immunoreactivity using an anti-Arc antibody (obtained from Santa Cruz) in home cage control (Ctrl) and pentylenetetrazole-injected (PTZ) groups (**a, upper panels**). Representative images of *Drd1*-tdTomato (red) and *Drd2*-GFP (green) labelled cells in Ctrl and PTZ groups of *B6.Cg-Tg(Drd1a-tdTomato)6Calak/J* x *Tg(Drd2-EGFP)S118Gsat* (GENSAT) dual-reporter mice (**a, lower panels**). Cumulative distribution of the average Arc intensity in *Drd1* and *Drd2* DLS cells, showing higher intensity in the PTZ than Ctrl group but no difference between *Drd1* and *Drd2* (**b**). Percentage of Arc-positive DLS cells (defined as those with an intensity above the threshold shown in the dashed line in panel b) in *Drd1*+ or *Drd2*+ DLS cells, showing a higher percentage in the PTZ than Ctrl group but no difference between *Drd1* and *Drd2* (**c**). Representative images of Arc immunoreactivity using an anti-Arc antibody (obtained from SYnaptic SYstems) in home cage control (Ctrl) and pentylenetetrazole-injected (PTZ) groups (**d, upper panels**). Representative images of *Drd1*-tdTomato (red) and *Drd2*-GFP (green) labelled cells in Ctrl and PTZ groups of *B6.Cg-Tg(Drd1a-tdTomato)6Calak/J* x *Tg(Drd2-EGFP)S118Gsat* dual-reporter mice (**d, lower panels**). Cumulative distribution of the average Arc intensity in *Drd1* and *Drd2* DLS cells, showing higher intensity in the PTZ than Ctrl group but no difference between *Drd1* and *Drd2* (**e**). Percentage of Arc-positive DLS cells (defined as those with an intensity above the threshold shown in the dashed line in panel b) in *Drd1*+ or *Drd2*+ DLS cells, showing a higher percentage in the PTZ than Ctrl group but no difference between *Drd1* and *Drd2* (**f**). Scale bars = 100 μm.

a

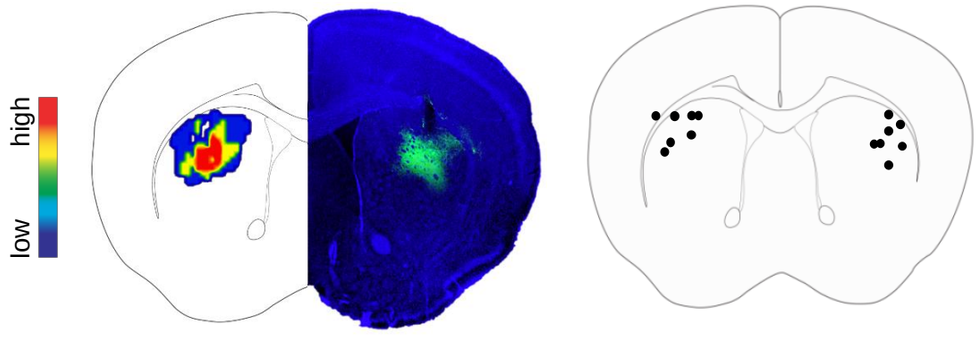

b

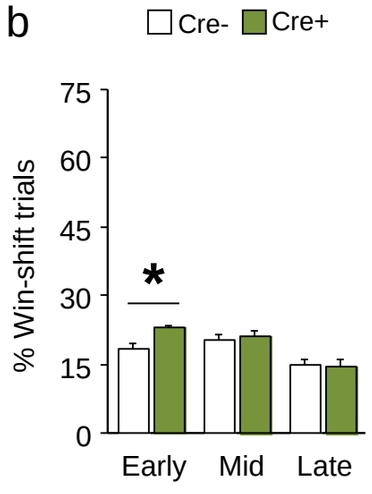

c

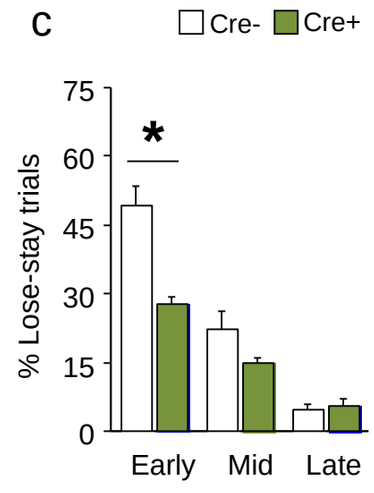

d

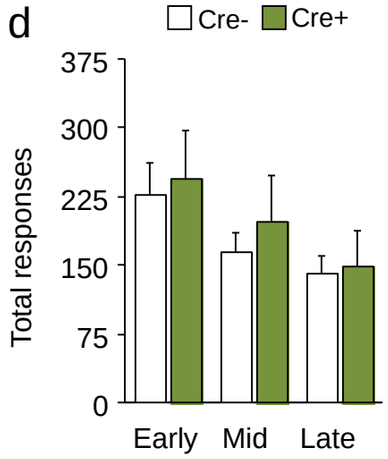

e

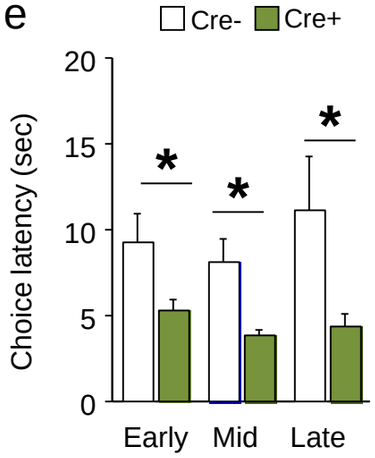

f

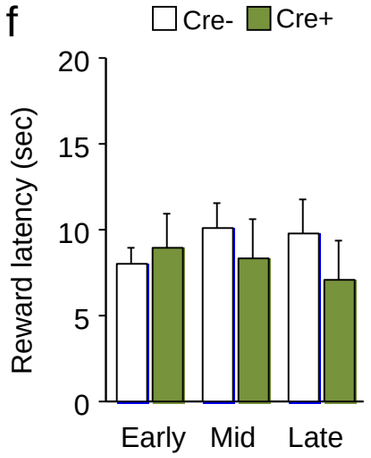

g

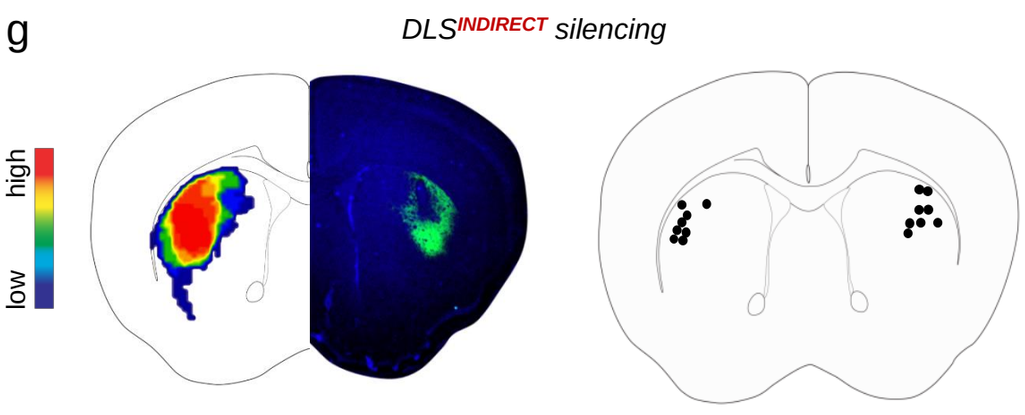

h

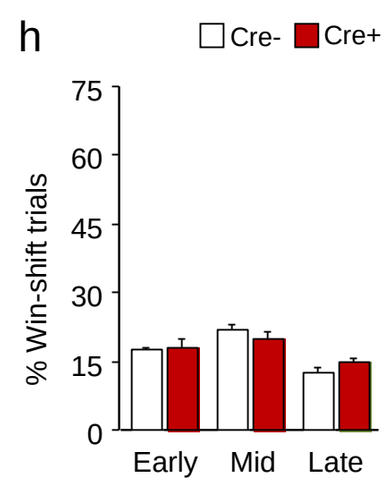

i

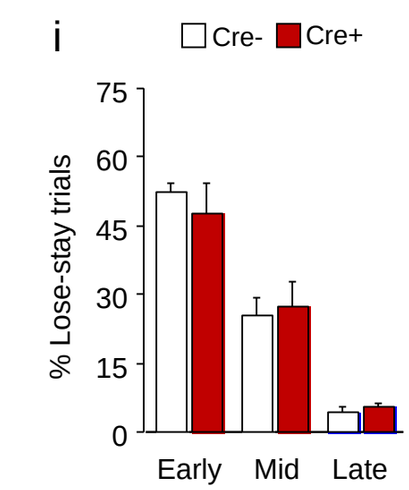

j

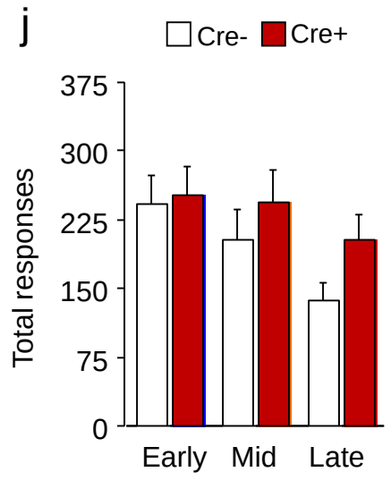

k

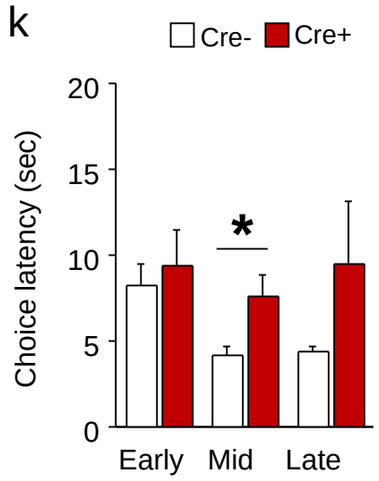

l

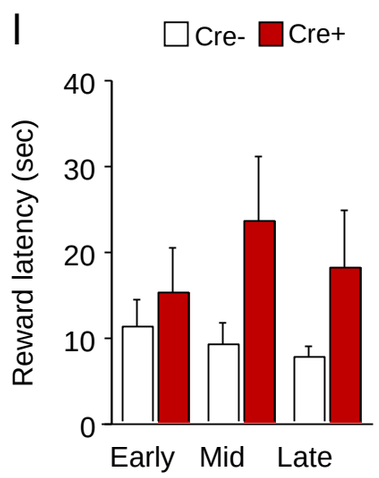

Figure S4: Effects of DLS direct- and indirect-pathway-photosilencing. Related to Figure 3. Example of virus localization and estimates of optical fiber placements (**a**). The Cre+ group had increased %win-stay trials (t(14)=2.85, *P*<0.05) (**b**) and decreased %lose-stay trials (t(14)=3.99, *P*<0.01) (**c**) than the Cre- group at early-learning. Total responses made did not differ between Cre+ and Cre- groups (**d**). The Cre+ group had faster response-latencies than the Cre- group at early (t(14)=2.34, *P*<.05), mid (t(14)=3.09, *P*<.01) and late (t(14)=2.27, *P*<.05) learning (**e**). Latency to collect reward did not differ between Cre+ and Cre- groups (**f**). Example of virus localization and estimates of optical fiber placements (**g**). Win-shift (**h**), and lose-stay (**i**) behavior did not differ between the Cre+ and Cre-groups. Total responses made did not differ between Cre+ and Cre- groups (**j**). The Cre+ group had slower response-latencies than the Cre- group at mid learning (t(14)=2.43, *P*<.05) (**k**). Latency to collect reward did not differ between Cre+ and Cre- groups (**l**). **P*<.05. Data are mean±SEM.

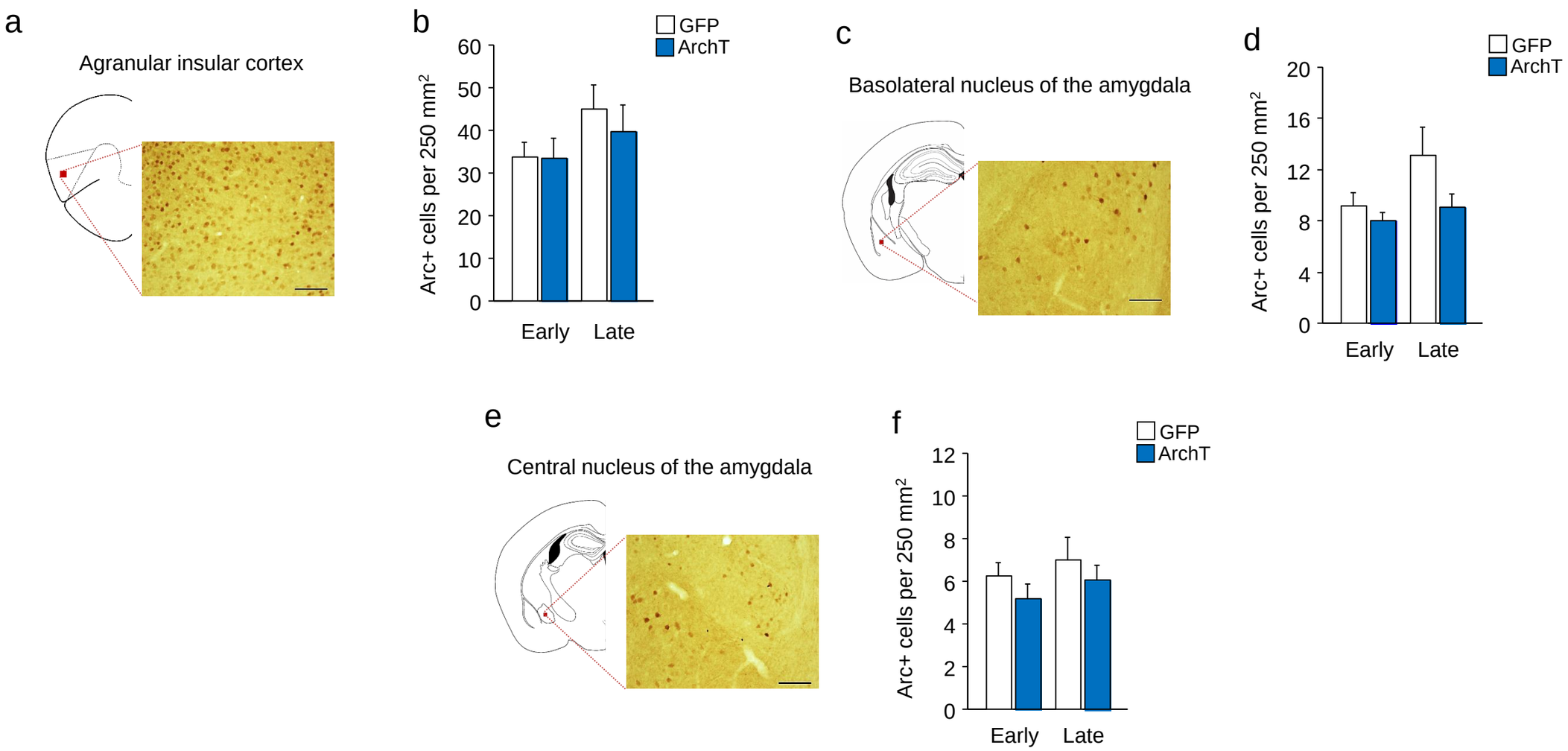

f

	Prelimbic cortex	Somatosensory cortex	Nucleus accumbens core	Nucleus accumbens shell	Agranular insular cortex	Basolateral amygdala	Central amygdala
Dorsomedial striatum	0.74 (*P*<.05)	0.38	0.50	0.44	0.35	0.17	0.15

Figure S5: System-level DLS-photosilencing effects. Related to Figure 4. Example of Arc-positive neurons in agranular insular cortex (**a**). Arc-positive neuron counts in agranular insular cortex did not differ between GFP and ArchT groups at early or late learning (group x stage ANOVA: *P*>.05) (**b**). Example of Arc-positive neurons in the basolateral nucleus of the amygdala (**c**). Arc-positive neuron counts in the basolateral nucleus of the amygdala did not differ between GFP and ArchT groups at early or late learning (group x stage ANOVA: *P*>.05) (**d**). Example of Arc-positive neurons in the central nucleus of the amygdala (**e**). Arc-positive neuron counts in the central nucleus of the amygdala did not differ between GFP and ArchT groups at early or late learning (group x stage ANOVA: *P*>.05) (**f**).

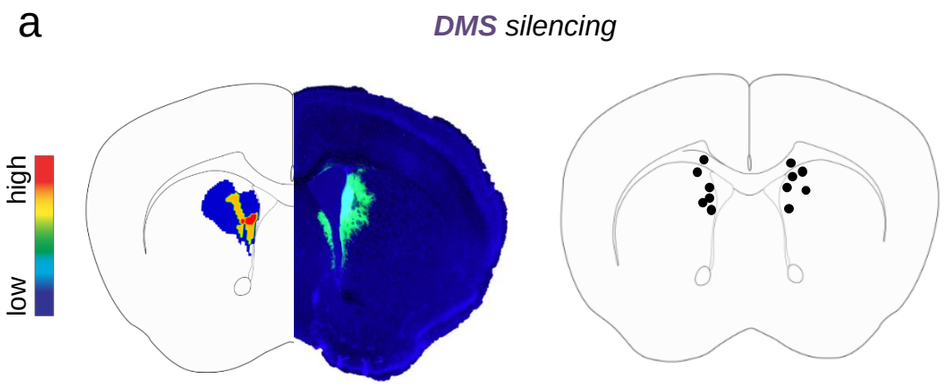
a
DMS silencing
high
low

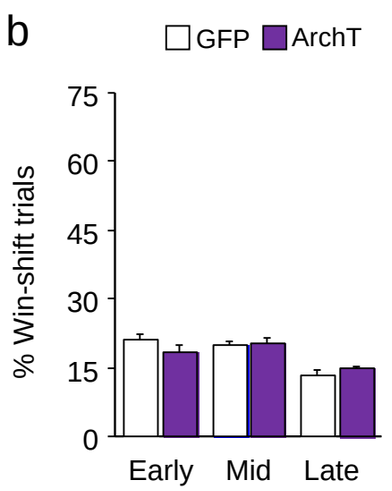
b
GFP
ArchT
% Win-shift trials
75
60
45
30
15
0
Early
Mid
Late

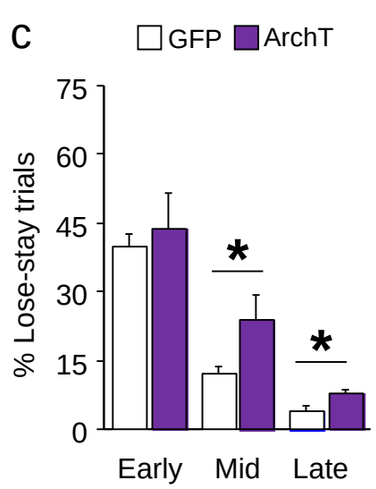
c
GFP
ArchT
% Lose-stay trials
75
60
45
30
15
0
*
*
Early
Mid
Late

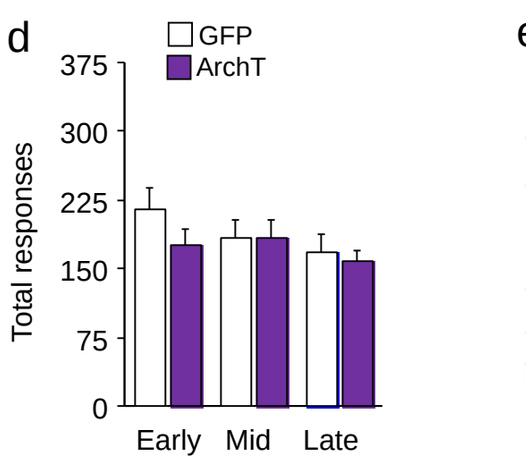
d
GFP
ArchT
Total responses
375
300
225
150
75
0
Early
Mid
Late

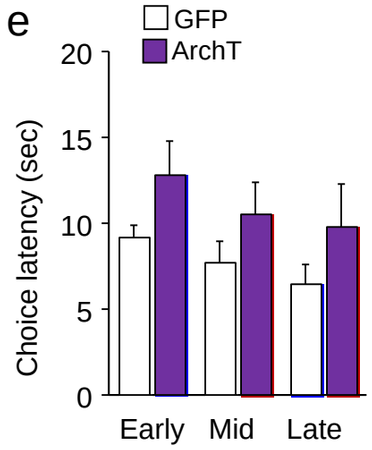
e
GFP
ArchT
Choice latency (sec)
20
15
10
5
0
Early
Mid
Late

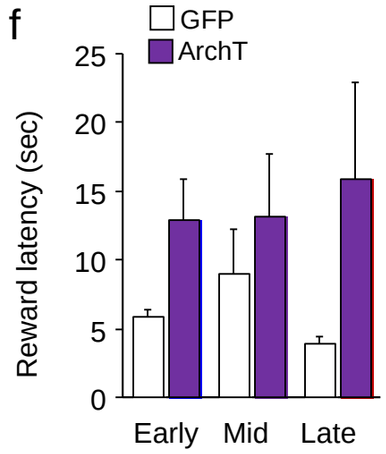
f
GFP
ArchT
Reward latency (sec)
25
20
15
10
5
0
Early
Mid
Late

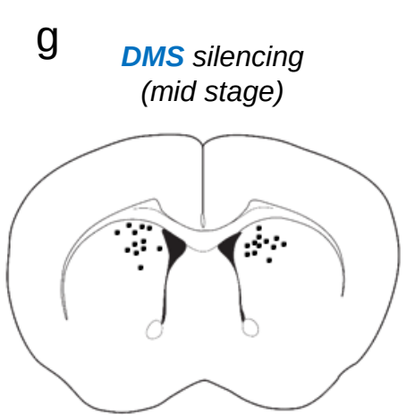
g
DMS silencing
(mid stage)

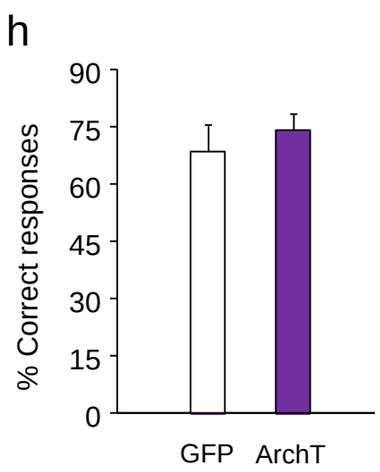
h
% Correct responses
90
75
60
45
30
15
0
GFP
ArchT

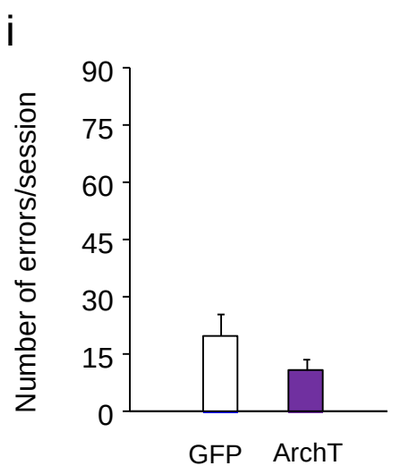
i
Number of errors/session
90
75
60
45
30
15
0
GFP
ArchT

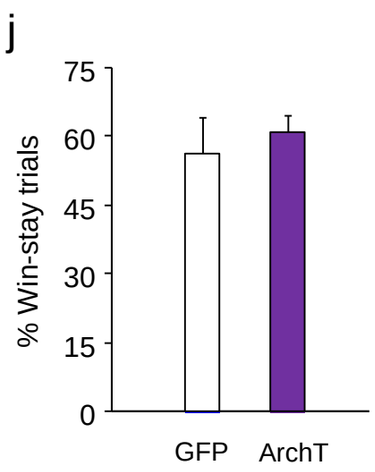
j
% Win-stay trials
75
60
45
30
15
0
GFP
ArchT

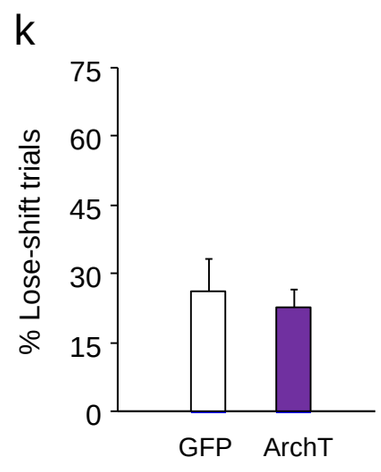
k
% Lose-shift trials
75
60
45
30
15
0
GFP
ArchT

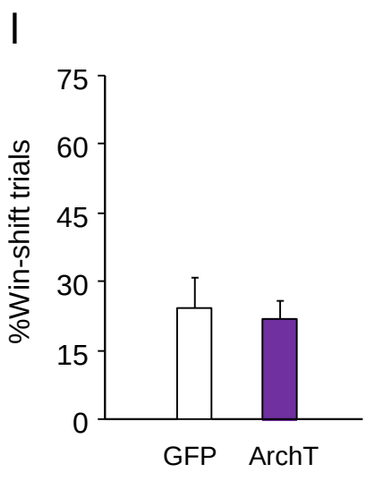
l
%Win-shift trials
75
60
45
30
15
0
GFP
ArchT

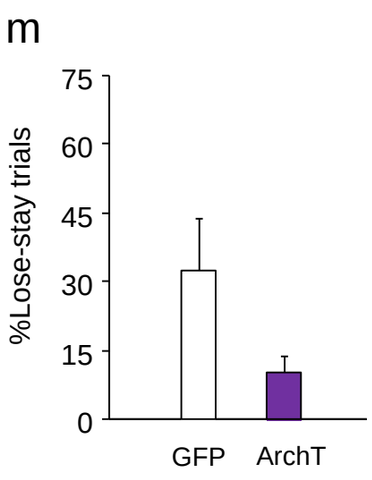
m
%Lose-stay trials
75
60
45
30
15
0
GFP
ArchT

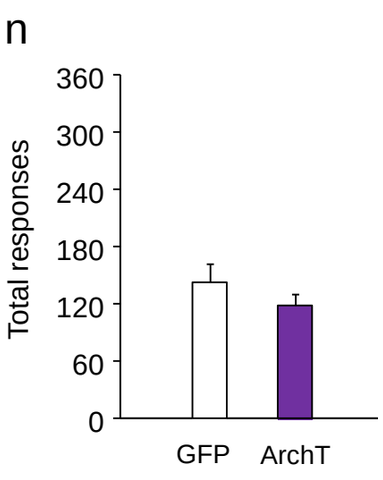
n
Total responses
360
300
240
180
120
60
0
GFP
ArchT

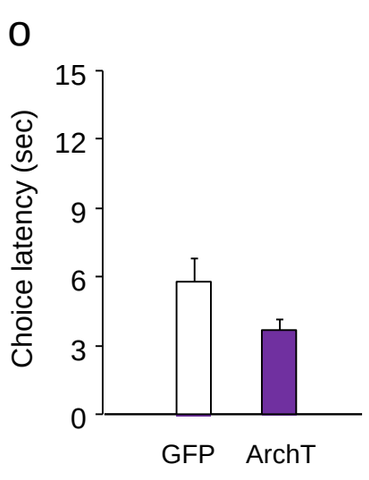
o
Choice latency (sec)
15
12
9
6
3
0
GFP
ArchT

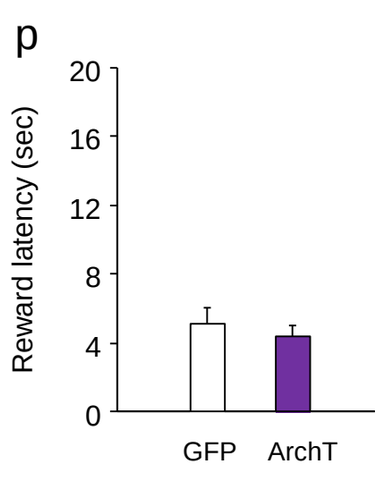
p
Reward latency (sec)
20
16
12
8
4
0
GFP
ArchT

Figure S6: Effects of DMS-photosilencing on auxiliary touchscreen-task measures and mid-stage learning. Related to Figure 4. Example of virus localization and estimates of optical fiber placements (**a**). %Win-stay trials did not differ between GFP and ArchT groups (**b**). The ArchT group had non-significantly increased %lose-stay trials at mid-learning ($t(14)=2.12$, $P=0.054$) and significantly increased %lose-stay trials late-learning ($t(14)=2.73$, $P<0.05$), as compared to the GFP group (**c**). Total responses made did not differ between GFP and ArchT groups (**d**). Choice latency did not differ between GFP and ArchT groups (**e**). Time to collect reward did not differ between GFP and ArchT groups (**f**). Estimates of optical fiber placements in the photosilencing at reward experiment (**g**). Percent correct responses did not differ between GFP and ArchT groups (n=5-7) (**h**). Errors-rates did not differ between GFP and ArchT groups (**i**). Win-stay (**j**), lose-shift (**k**), win-shift (**l**), and lose-stay (**m**) behavior did not differ between GFP and ArchT groups. Total responses did not differ between GFP and ArchT groups (**n**). Choice latency did not differ between GFP and ArchT groups (**o**). Latency to collect reward did not differ between GFP and ArchT groups (**p**). All measures: group x stage ANOVA: $P>.05$. Data are mean±SEM.